

Published in final edited form as:

Curr Biol. 2015 February 2; 25(3): 379–384. doi:10.1016/j.cub.2014.11.066.

Proteomic Analysis of Isolated Ciliary Transition Zones Reveals the Presence of ESCRT Proteins

Dennis R. Diener^{1,*}, Pietro Lupetti², and Joel L. Rosenbaum^{1,*}

¹Department of Molecular, Cellular and Developmental Biology, Yale University, New Haven, CT, 06511, USA

²Department of Life Sciences, University of Siena, Siena, 53100, Italy

Summary

The transition zone (TZ) is a specialized region of the cilium characterized by Y-shaped connectors between the microtubules of the ciliary axoneme and the ciliary membrane [1]. Located near the base of the cilium (Fig. 1A), the TZ is in the prime location to act as a gate for proteins into and out of the ciliary compartment, a role supported by experimental evidence [2-6]. The importance of the TZ has been underscored by studies showing that mutations affecting proteins located in the TZ result in cilia-related diseases, or ciliopathies, presenting symptoms including renal cysts, retinal degeneration, and situs inversus [7-9]. Some TZ proteins have been identified and shown to interact with each other through coprecipitation studies in vertebrate cells [4, 10, 11] and genetics studies in *C. elegans* [3]. As a distinct approach to identify TZ proteins we have taken advantage of the biology of *Chlamydomonas* to isolate TZs. Proteomic analysis identified 115 proteins, 10 of which were known TZ proteins related to ciliopathies, indicating that the preparation was highly enriched for TZs. Interestingly, six proteins of the endosomal sorting complexes required for transport (ESCRT) were also associated with the TZs. Identification of these and other proteins in the TZ will provide new insights into functions of the TZ as well as candidate ciliopathy genes.

Results and Discussion

Isolation of transition zones

The TZ of *Chlamydomonas* is demarcated by a distinctive nine-pointed star (stellate structure) with a cylinder at its center that looks like an “H” in longitudinal section (Figs. 1A) [12, 13]. Although the stellate structure and central cylinder are not present in vertebrate cilia, the proximal region of the cilia of *Chlamydomonas* and vertebrates do have structures (e.g. “Y” connectors Fig. 2H [12-14]) and proteins (e.g., CEP290 [2, 4]) in common.

© 2014 Elsevier Ltd. All rights reserved.

*Correspondence: dennis.diener@yale.edu, joel.rosenbaum@yale.edu.

Publisher's Disclaimer: This is a PDF file of an unedited manuscript that has been accepted for publication. As a service to our customers we are providing this early version of the manuscript. The manuscript will undergo copyediting, typesetting, and review of the resulting proof before it is published in its final citable form. Please note that during the production process errors may be discovered which could affect the content, and all legal disclaimers that apply to the journal pertain.

Determining the makeup of *Chlamydomonas* TZs, therefore, should provide new insights into the composition and function of vertebrate TZs.

The life cycle of *Chlamydomonas* provided a means to isolate the TZ from this biflagellate alga. Before cell division, *Chlamydomonas* resorbs its flagella: the flagella gradually shorten, finally detaching from the basal body, leaving a vesicle containing the central cylinder of the TZ as the last remnant of the flagellum (Fig. 1B)[15-17]. This vesicle, referred to hereafter as the TZ, sometimes remains entrapped in the flagellar collar [15, 17], a proteinaceous sheath [18] that forms a channel through the cell wall for the flagellum (Fig. 1A). To determine how prevalent the vesicles were in flagellar collars, isolated cell walls were stained for acetylated α -tubulin and the flagellar collar. Many cell walls contained a pair of flagellar collars with a punctum of acetylated α -tubulin, representing a TZ, within each collar (Fig. 1C and D). CEP290, a known component of the TZ [2], was also present in many of the TZs (Fig. 1E).

To isolate TZs, cell walls were fractionated on cesium chloride gradients producing a band in the lower third of the gradient containing flagellar collars as previously described [18]. Electron microscopy of negative stained samples from this band revealed that the flagellar collars retained electron dense vesicles (Fig. 2A and B). After extraction with NP-40, the central cylinder characteristic of the TZ could be seen (Fig. 2C), confirming that these vesicles were TZs. Treatment of the crude preparation of TZs with gamete lytic enzyme to break down cell wall material before separation on the cesium chloride gradient, released the TZs from the flagellar collars (Fig. S1). TZs from the cesium chloride gradient were further purified on an iodixanol (Optiprep) step gradient (see Experimental Procedures). The 60%-30% interface of the iodixanol gradient was sedimented and appeared to contain predominantly TZs by DIC microscopy (Figs. S1C and D).

Ultrastructure of the isolated TZ

The isolated TZs were examined by transmission electron microscopy of thin sections (Fig. 2D-F) as well as by electron tomography of thick sections (Fig. 2G). Electron tomographic reconstructions of TZs *in situ* illustrate the stellate structure surrounding the central cylinder, with its apexes attached to the outer doublet microtubules (Fig. 2H). Y-shaped connectors can also be seen between the outer doublet microtubules and the membrane (Fig. 2H, arrows). In the isolated TZs, the outer doublet microtubules had depolymerized and the stellate structure was not identifiable. Still, the central cylinders remained intact although the transverse plate that separates the proximal and distal cylinders was missing (Fig. 2E, arrow). Thus, the central cylinder is an autonomous structure whose integrity is not dependent on the stellate fibers (Fig. 2E-G, Movie S1).

Nine projections extended from the central cylinder toward the outer membrane (Fig. 2F and G, Movie S1). In favorable sections, especially in the sectioned tomograms, these projections appeared to form Y-shaped attachments to the membrane (Fig. 2G, arrows). (The coarser appearance of the filaments in the isolated TZs compared to the *in situ* TZ may be due, in part, to the inclusion of tannic acid in the fixation of the former.)

Sections that cut through the periphery of the TZ showed a cross hatched pattern (Fig. 2D, arrows) indicating that membrane-associated proteins retained an ordered longitudinal and circumferential pattern on the inner surface of the TZ vesicles even in the absence of microtubules. The longitudinal arrays are likely formed by the Y-shaped connectors, which in the flagella are aligned with the outer doublet microtubules. The origin of the circumferential pattern is less clear; it may be a manifestation of the wedge connectors (Fig. 1A).

Analysis of the isolated TZs by SDS-PAGE showed their composition was very different from whole flagella (Fig. S2). Potential contaminating proteins of cell walls were not prominent in the TZs. Centrin, a known component of the TZ [19] was highly enriched in this fraction as seen on a silver stained gel (Fig. S2A) and by immunoblotting (Fig. S2B). The preparation appeared to contain little contamination from flagella or cell walls, and was deemed suitable for proteomic analysis.

Proteomic analysis of transition zones

The protein composition of the isolated TZs was analyzed by mass spectrometry; proteins identified with at least two peptides and >90% probability were accepted (Table S1). No ribosomal proteins or components of the chloroplast were found in this protein set, although three ribosomal subunits were identified with a single peptide (Table S2), indicating that cytoplasmic contamination was minimal. Likewise, no hydroxyproline-rich proteins or pterophorins, characteristic of the cell wall, were identified in the TZ proteome. Axonemal dyneins and radial spokes, which are only present on the axoneme distal to the TZ, were not identified by two peptides, indicating that few flagella were present in the TZs preparation. Furthermore, despite the fact that the isolated TZs were generated by the resorption of flagella prior to division, disassembled components of the depolymerizing axoneme were not prominent contaminants of the TZs.

Forty-nine of the proteins in the TZ proteome were also present in the *Chlamydomonas* flagellar proteome [20] (Table S1). In addition, three Bardet Biedl Syndrome (BBS) proteins, BBS1, BBS7 and BBS8, present in *Chlamydomonas* flagella [21] but not in the flagellar proteome, were present. Many of these 52 flagellar proteins, e.g. α - and α -tubulin and the major flagellar membrane glycoprotein FMG1, have a general flagellar function rather than a TZ specific function. Others may have distinct roles in TZs and flagella: centrin, for example, is a known component of the central cylinder in TZs [19], whereas in flagella it is a subunit of inner arm dynein.

In addition to centrin, other known TZ proteins identified included a class of proteins associated with the nephronophthisis/Meckel Syndrome/Joubert Syndrome family of ciliopathies [8, 9, 22]. Fourteen homologues of this class of protein were identified in the predicted proteome of *Chlamydomonas* [23]. Of these, nine were identified in the TZ proteome (Table S3). In addition, a protein with limited similarity to NPHP1 was also present. This protein fell below the e-value cut off ($1e^{-5}$) used by Barker et al. [23] when searching for *Chlamydomonas* homologues, but a pair-wise BLAST alignment of the *Chlamydomonas* and *H. sapiens* proteins gave an e-value of $8e^{-10}$, suggesting that this is the *Chlamydomonas* NPHP1 homologue. Four *Chlamydomonas* homologues of the MKS and

NPHP complex proteins, R PGRIPL1, TMEM216, TMEM237, and B9D1 [23], were not identified, suggesting that either the current proteome is not complete or these proteins were missing from the isolated TZs. Other putative TZ proteins identified include the two subunits of katanin, one of which was previously shown to be present in the TZ [24], and Fa1, which is involved in flagellar autotomy (the severing of the flagellum just distal to the TZ) and was hypothesized to be in the TZ [25].

Of the remaining proteins, 32 were predicted proteins with little similarity to vertebrate proteins (Table S1). The remaining 18 proteins were newly identified as being associated with the TZ of *Chlamydomonas* and had strong similarity to human proteins (Table 1). These proteins include two large proteins with multiple Polycystin-1, Lipoxygenase, Alpha-Toxin (PLAT) domains (POC2 and Mot51), a lipid flipase, an A-type cyclin, a cyclin-dependent kinase, and six proteins of the endosomal sorting complexes required for transport (ESCRT) system (Table 1). To validate two of these putative TZ proteins, antibodies were generated against POC2 and one ESCRT protein, VPS4. Immunofluorescence of flagella/basal body complexes and isolated cell walls containing TZs confirmed that these proteins were located at the base of the flagella and in the TZ (Fig. 3). VPS4 previously has been found at the centrosome of tissue culture cells [26].

Nucleoporins and the TZ

Trafficking of proteins into and out of the cilium has been compared to transport through the nuclear pore [27, 28]. The ciliary pore complex (CPC) may share size exclusion characteristics with the nuclear pore [29, 30], and soluble proteins that shuttle cargo into and out of the nucleus, i.e. Ran, importins, and exportin, have been found to be associated with cilia and centrosomes (Wu, H., Pazour, G.J., Witman, G.B., and Rosenbaum, J.L. (2004). The small GTPase Ran is localized to the flagella in *Chlamydomonas reinhardtii*. Mol. Biol. Cell 15, 409a (abstract); Tsao, C., Wood, C.R., and Rosenbaum, J.L. (2008). The small GTPase Ran and nuclear transport adapter protein importin-alpha are present in the flagella in *Chlamydomonas reinhardtii*. Mol. Biol. Cell 19 (suppl.), abstract #1041[20, 31-34]. Furthermore, nucleoporins, components of the nuclear pore, have been found at the base of cilia [29] and experimentally induced dimerization of NUP64, a central component of the nucleopore, inhibits entry of nonmembrane proteins into the nucleus and cilium [35]. Because no nucleoporin was identified in the TZ proteome it seems unlikely they are a prominent feature of the TZ in *Chlamydomonas*. However, they may be located proximal to the TZ, surrounding the basal body, as has been suggested in mammalian cells [35].

ESCRT proteins are associated with the TZ

Interestingly, six ESCRT-related proteins were identified in the TZ proteome (Table 1). The ESCRT machinery comprises several complexes (ESCRT 0-III, Vps4 complex) and accessory proteins (e.g. Alix) involved in membrane fission events that could be important for ciliary membrane dynamics. First, ESCRT proteins shuttle ubiquitinated proteins into multivesicular bodies [36] and could serve this function at the base of flagella, especially during flagellar resorption when ubiquitination of flagellar proteins increases dramatically [37]. Second, ESCRT proteins are required for the final abscission of the midbody to complete cytokinesis [38] and could participate in the topologically similar processes of

flagellar autotomy and the pinching off of the TZ vesicle that occurs prior to cell division. Third, the ESCRT machinery provides the mechanism for the budding of vesicles (ectosomes) from the cell surface [39]. *Chlamydomonas* flagella release ectosomes [40] and such ectosomes are active in breaking down the mother cell wall following cell division [41]. Ectosomes may be released continuously from all cilia, and ESCRT is the only mechanism known to facilitate the outward budding of membrane.

The TZ vesicles isolated in this study were formed by flagellar resorption and fission of the TZ vesicle from the cell membrane prior to cell division. The presence of ESCRT proteins in these TZs may be related to these division-specific functions. Identification of VPS4 in isolated flagella/basal body complexes of non-dividing cells (Fig. 3), however, suggests these proteins are always present at the base of cilia.

Other evidence also suggests that ESCRT proteins are involved in ciliary function. Table 4S lists the results of a search for homologues of ESCRT proteins in *Chlamydomonas* in the cilia database Cildb [42]. Of the 14 ESCRT proteins identified in the *Chlamydomonas* genome, 6 were present in the TZ proteome and 10 have been identified in at least one other study of ciliary or centrosomal proteins (Table 4S). In addition, a comparison of the protein composition of flagellar membrane to that of vesicles released from *Chlamydomonas* flagella showed a heightened concentration of ALIX in the vesicles, consistent with the involvement of the ESCRT machinery in formation of flagellar ectosomes (K. Huang and JLR, unpublished). Furthermore, ESCRT protein VPS4 has been detected associated with the centrosome and its knockdown affects centriole duplication [26]. Finally, ESCRT 0 proteins are found at the base of sensory cilia of *C. elegans* where they modulate the amount of LOV-1 and PKD2 in cilia [43]. Thus, evidence from widespread sources suggests that the ESCRT machinery is associated with the ciliary apparatus.

Membrane trafficking plays an important role in the formation and function of cilia [9, 41, 44-48] and the ESCRT machinery may be a previously unrecognized component involved in the dynamics of the ciliary membrane. Identification of ESCRT proteins associated with the TZ of *Chlamydomonas*, along with other proteins identified in the TZ proteome, provides new clues to the functions of cilia and their involvement in ciliopathies.

Experimental Procedures

Purification of TZs

For initial experiments cell walls were isolated from *pf18* mt- cells. This paralyzed flagella mutant often fails to hatch and the daughter cells accumulate inside the mother cell wall. When resuspended in 10 mM Hepes pH 7.4, the daughter cells hatch but the walls from which they escaped remain partially intact in the medium. When the hatched cells and walls are centrifuged at $12,000 \times g$ the cells form a stable pellet covered by the flocculent cell walls, which can be resuspended by gently shaking the centrifuge tube [49]. After several rounds of centrifugation and resuspension in 10 mM Hepes pH 7.4, 5 mM $MgCl_2$, 0.5 mM EGTA, 1 mM DTT, and 25 mM KCl (HMDEK) the cell walls were freed of most of the cells. Cesium chloride gradients had been used previously to purify cell walls [49] and flagellar collars [18]. (Interestingly, in 1975 Hills et al. noted that a minor component on

such gradients consisted of “0.5 μm diameter circular amorphous objects of unknown composition” that were also seen “in close association with the basal end of the flagellar collars.” [49]). The suspension of walls was brought to a final volume of 4.5 ml of 2.8 M cesium chloride and was centrifuged in an SW55 rotor (Beckman) at 38,000 rpm for 14 hr. This led to a band of flagellar collars that contained TZs (Fig. 2). Later preparations were made with *pf1* mt- cells. These cells, like *pf18* cells, often fail to hatch after division, but when the cells are hatched in 10 mM Hepes pH 7.4, unlike *pf18*, the walls disappear microscopically, presumably degraded more completely by the hatching protease, vegetative lytic enzyme (VLE). After hatching in 10 mM Hepes pH 7.4, the cells were removed by centrifuging twice at $500 \times g$ for 10 min, and the supernatant was centrifuged at $23,500 \times g$ for 30 min. The resulting pellets were resuspended in HMDEK and residual cells were removed by centrifugation through a 25% sucrose cushion ($500 \times g$ for 10 min). The supernatant was centrifuged at $135,000 \times g$ for 30 min and the pellet was resuspended in 2 ml of gamete lytic enzyme (GLE or autolysin). After incubation for 1-2 hr at room temperature the preparation was separated on a cesium chloride gradient as described above. Often preparations from two consecutive days starting with 32 liters of cells each day were combined on a single gradient. After centrifugation the gradient had three major bands enriched in flagella, transition zones, and empty flagellar collars (Fig. S1). The band containing transition zones was diluted 1:1 with HMDEK and was centrifuged at 75,000 rpm in a TLA120.2 rotor (Beckman) for 20 min. The resulting pellet was resuspended in 0.5 ml HMDEK and was mixed with an equal volume of 60% iodixanol (Optiprep). This formed the middle layer of a 60, 30, 20% iodixanol step gradient, which was centrifuged for 3 hr at 50,000 rpm in a TLS55 rotor (Beckman). Flagella and other membranous contaminants accumulated at the 30%/20% interface. TZs were collected from the 60%/30% interface, diluted and sedimented as above in a TLA120.2 rotor (Figs. 2, S1C and D).

Supplemental Experimental Procedures

Please see the Supplemental Experimental Procedures for a description of light and electron microscopy techniques, proteomic analysis, and other experimental procedures.

Supplementary Material

Refer to Web version on PubMed Central for supplementary material.

Acknowledgements

This work was initiated through a collaboration [17] with Lynne Quarmby, who brought to our attention the release of TZs from dividing cells. The authors are grateful to Hue Tran for invaluable help in preparing transition zones and Mariangela Gentile and Eugenio Paccagnini for their collaboration on electron tomography of both in situ and isolated TZs. Thanks also to Todd Markowski and LeeAnn Higgins for performing the mass spectrometry analysis. We also thank Branch Craige, George Witman and Jeff Salisbury for the CEP290 and centrin antibodies. The work was supported by NIH grant GM014642 to J.L.R.

References

1. Gilula N, Satir P. The ciliary necklace. A ciliary membrane specialization. *J. Cell Biol.* 1972; 53:494–509. [PubMed: 4554367]

2. Craige B, Tsao CC, Diener DR, Hou Y, Lechtreck KF, Rosenbaum JL, Witman GB. CEP290 tethers flagellar transition zone microtubules to the membrane and regulates flagellar protein content. *J. Cell Biol.* 2010; 190:927–940. [PubMed: 20819941]
3. Williams CL, Li C, Kida K, Inglis PN, Mohan S, Semenec L, Bialas NJ, Stupay RM, Chen N, Blacque OE, et al. MKS and NPHP modules cooperate to establish basal body/transition zone membrane associations and ciliary gate function during ciliogenesis. *J. Cell Biol.* 2011; 192:1023–1041. [PubMed: 21422230]
4. Garcia-Gonzalo FR, Corbit KC, Sinerol-Piquer MS, Ramaswami G, Otto EA, Noriega TR, Seol AD, Robinson JF, Bennett CL, Josifova DJ, et al. A transition zone complex regulates mammalian ciliogenesis and ciliary membrane composition. *Nat. Genet.* 2011; 43:776–784. [PubMed: 21725307]
5. Hu Q, Nelson WJ. Ciliary diffusion barrier: the gatekeeper for the primary cilium compartment. *Cytoskeleton.* 2011; 68:313–324. [PubMed: 21634025]
6. Reiter JF, Blacque OE, Leroux MR. The base of the cilium: roles for transition fibres and the transition zone in ciliary formation, maintenance and compartmentalization. *EMBO Rep.* 2012; 13:608–618. [PubMed: 22653444]
7. Tobin JL, Beales PL. The nonmotile ciliopathies. *Genet. Med.* 2009; 11:386–402. [PubMed: 19421068]
8. Szymanska K, Johnson CA. The transition zone: an essential functional compartment of cilia. *Cilia.* 2012; 1:10. [PubMed: 23352055]
9. Madhivanan K, Aguilar RC. Ciliopathies: the trafficking connection. *Traffic.* 2014; 15:1031–1056. [PubMed: 25040720]
10. Sang L, Miller JJ, Corbit KC, Giles RH, Brauer MJ, Otto EA, Baye LM, Wen X, Scales SJ, Kwong M, et al. Mapping the NPHP-JBTS-MKS protein network reveals ciliopathy disease genes and pathways. *Cell.* 2011; 145:513–528. [PubMed: 21565611]
11. Chih B, Liu P, Chinn Y, Chalouni C, Komuves LG, Hass PE, Sandoval W, Peterson AS. A ciliopathy complex at the transition zone protects the cilia as a privileged membrane domain. *Nat. Cell Biol.* 2012; 14:61–72. [PubMed: 22179047]
12. Ringo DL. Flagellar motion and fine structure of the flagellar apparatus in *Chlamydomonas*. *J. Cell Biol.* 1967; 33:543–571. [PubMed: 5341020]
13. Geimer S, Melkonian M. The ultrastructure of the *Chlamydomonas reinhardtii* basal apparatus: identification of an early marker of radial asymmetry inherent in the basal body. *J. Cell Sci.* 2004; 117:2663–2674. [PubMed: 15138287]
14. Anderson RGW, Hein CE. Distribution of anionic sites on the oviduct ciliary membrane. *J. Cell Biol.* 1977; 72:482–492. [PubMed: 833205]
15. Cavalier-Smith T. Basal body and flagellar development during the vegetative cell cycle and the sexual cycle of *Chlamydomonas reinhardtii*. *J. Cell Sci.* 1974; 16:529–556. [PubMed: 4615103]
16. Gaffal KP. The basal body-root complex of *Chlamydomonas reinhardtii* during mitosis. *Protoplasma.* 1988; 143:118–129.
17. Parker JD, Hilton LK, Diener DR, Rasi MQ, Mahjoub MR, Rosenbaum JL, Quarmby LM. Centrioles are freed from cilia by severing prior to mitosis. *Cytoskeleton.* 2010; 67:425–430. [PubMed: 20506243]
18. Snell WJ. Characterization of the *Chlamydomonas* flagellar collar. *Cell Motil. Cytoskeleton.* 1983; 3:273–280.
19. Sanders MA, Salisbury JL. Centrin-mediated microtubule severing during flagellar excision in *Chlamydomonas reinhardtii*. *J. Cell Biol.* 1989; 108:1751–1760. [PubMed: 2654141]
20. Pazour G, Agrin N, Leszyk J, Witman G. Proteomic analysis of a eukaryotic cilium. *J. Cell Biol.* 2005; 170:103–113. [PubMed: 15998802]
21. Lechtreck KF, Johnson EC, Sakai T, Cochran D, Ballif BA, Rush J, Pazour GJ, Ikebe M, Witman GB. The *Chlamydomonas reinhardtii* BBSome is an IFT cargo required for export of specific signaling proteins from flagella. *J. Cell Biol.* 2009; 187:1117–1132. [PubMed: 20038682]
22. Czarnecki PG, Shah JV. The ciliary transition zone: from morphology and molecules to medicine. *Trends Cell Biol.* 2012; 22:201–210. [PubMed: 22401885]

23. Barker AR, Renzaglia KS, Fry K, Dawe HR. Bioinformatic analysis of ciliary transition zone proteins reveals insights into the evolution of ciliopathy networks. *BMC Genomics*. 2014; 15:531. [PubMed: 24969356]
24. Lohret TA, Zhao L, Quarmby LM. Cloning of *Chlamydomonas* p60 katanin and localization to the site of outer doublet severing during deflagellation. *Cell Motil. Cytoskeleton*. 1999; 43:221–231. [PubMed: 10401578]
25. Finst RJ, Kim PJ, Griffis ER, Quarmby LM. Fa1p is a 171 kDa protein essential for axonemal microtubule severing in *Chlamydomonas*. *J. Cell Sci*. 2000; 113:1963–1971. [PubMed: 10806107]
26. Morita E, Colf LA, Karren MA, Sandrin V, Rodesch CK, Sundquist WI. Human ESCRT-III and VPS4 proteins are required for centrosome and spindle maintenance. *Proc. Natl. Acad. Sci. U S A*. 2010; 107:12889–12894. [PubMed: 20616062]
27. Rosenbaum JL, Witman GB. Intraflagellar Transport. *Nature Rev. Cell Mol. Biol*. 2002; 3:813–825.
28. Kee HL, Verhey KJ. Molecular connections between nuclear and ciliary import processes. *Cilia*. 2013; 2:11. [PubMed: 23985042]
29. Kee HL, Dishinger JF, Blasius TL, Liu CJ, Margolis B, Verhey KJ. A size-exclusion permeability barrier and nucleoporins characterize a ciliary pore complex that regulates transport into cilia. *Nat. Cell Biol*. 2012; 14:431–437. [PubMed: 22388888]
30. Breslow DK, Koslover EF, Seydel F, Spakowitz AJ, Nachury MV. An in vitro assay for entry into cilia reveals unique properties of the soluble diffusion barrier. *J. Cell Biol*. 2013; 203:129–147. [PubMed: 24100294]
31. Fan S, Fogg V, Wang Q, Chen XW, Liu CJ, Margolis B. A novel Crumbs3 isoform regulates cell division and ciliogenesis via importin beta interactions. *J. Cell Biol*. 2007; 178:387–398. [PubMed: 17646395]
32. Fan S, Margolis B. The Ran importin system in cilia trafficking. *Organogenesis*. 2011; 7:147–153. [PubMed: 21791971]
33. Andersen JS, Wilkinson CJ, Mayor T, Mortensen P, Nigg EA, Mann M. Proteomic characterization of the human centrosome by protein correlation profiling. *Nature*. 2003; 426:570–574. [PubMed: 14654843]
34. Liu Q, Tan G, Levenkova N, Li T, Pugh EN Jr, Rux JJ, Speicher DW, Pierce EA. The proteome of the mouse photoreceptor sensory cilium complex. *Mol. Cell. Proteomics*. 2007; 6:1299–1317. [PubMed: 17494944]
35. Takao D, Dishinger JF, Kee HL, Pinskey JM, Allen BL, Verhey KJ. An assay for clogging the ciliary pore complex distinguishes mechanisms of cytosolic and membrane protein entry. *Curr. Biol*. 2014; 24:2288–2294. [PubMed: 25264252]
36. Bissig C, Gruenberg J. ALIX and the multivesicular endosome: ALIX in Wonderland. *Trends Cell Biol*. 2014; 24:19–25. [PubMed: 24287454]
37. Huang K, Diener DR, Rosenbaum JL. The ubiquitin conjugation system is involved in the disassembly of cilia and flagella. *J. Cell Biol*. 2009; 186:601–613. [PubMed: 19704024]
38. Caballe A, Martin-Serrano J. ESCRT machinery and cytokinesis: the road to daughter cell separation. *Traffic*. 2011; 12:1318–1326. [PubMed: 21722282]
39. Nabhan JF, Hu R, Oh RS, Cohen SN, Lu Q. Formation and release of arrestin domain-containing protein 1-mediated microvesicles (ARMMs) at plasma membrane by recruitment of TSG101 protein. *Proc. Natl. Acad. Sci USA*. 2012; 109:4146–4151. [PubMed: 22315426]
40. Bergman K, Goodenough UW, Goodenough DA, Jawitz J, Martin H. Gametic differentiation in *Chlamydomonas reinhardtii*. II. Flagellar membranes and the agglutination reaction. *J. Cell Biol*. 1975; 67:606–622. [PubMed: 1202016]
41. Wood CR, Huang K, Diener DR, Rosenbaum JL. The cilium secretes bioactive ectosomes. *Curr. Biol*. 2013; 23:906–911. [PubMed: 23623554]
42. Arnaiz O, Malinowska A, Klotz C, Sperling L, Dadlez M, Koll F, Cohen J. Cildb: a knowledgebase for centrosomes and cilia. *Database (Oxford)*. 2009; 2009:bap022. [PubMed: 20428338]
43. Hu J, Wittekind SG, Barr MM. STAM and Hrs down-regulate ciliary TRP receptors. *Mol. Biol. Cell*. 2007; 18:3277–3289. [PubMed: 17581863]

44. Kaplan OI, Doroquez DB, Cevik S, Bowie RV, Clarke L, Sanders AA, Kida K, Rappoport JZ, Sengupta P, Blacque OE. Endocytosis genes facilitate protein and membrane transport in *C. elegans* sensory cilia. *Curr. Biol.* 2012; 22:451–460. [PubMed: 22342749]
45. Clement CA, Ajbro KD, Koefoed K, Vestergaard ML, Veland IR, Henriques de Jesus MP, Pedersen LB, Benmerah A, Andersen CY, Larsen LA, et al. TGF-beta signaling is associated with endocytosis at the pocket region of the primary cilium. *Cell Rep.* 2013; 3:1806–1814. [PubMed: 23746451]
46. Sung CH, Leroux MR. The roles of evolutionarily conserved functional modules in cilia-related trafficking. *Nat. Cell Biol.* 2013; 15:1387–1397. [PubMed: 24296415]
47. Dentler W. A role for the membrane in regulating *Chlamydomonas* flagellar length. *PloS one.* 2013; 8:e53366. [PubMed: 23359798]
48. Wood CR, Rosenbaum JL. Proteins of the ciliary axoneme are found on cytoplasmic membrane vesicles during growth of cilia. *Curr. Biol.* 2014; 24:1114–1120. [PubMed: 24814148]
49. Hills GJ, Phillips JM, Gay MR, Roberts K. Self-assembly of a plant cell wall in vitro. *J. Mol. Biol.* 1975; 96:431–441. [PubMed: 1100848]

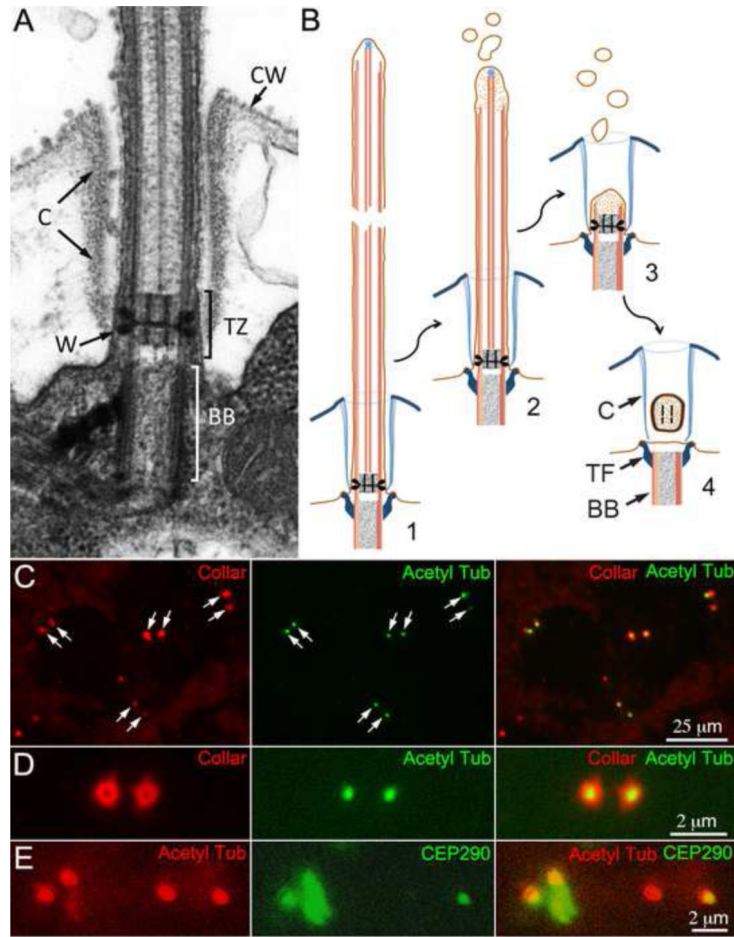


Figure 1.

A. Electron micrograph of the transition zone. The transition zone (TZ) of *Chlamydomonas* is characterized by a bipartite cylinder bisected by a transverse plate, which together look like an “H” in midsagittal section. Electron dense wedge connectors (W) extend from the axonemal microtubules to the membrane. The flagella pass through a flagellar collar (C) to exit the cell wall (CW). B. Diagram of the formation of the TZ vesicle. 1-3. Prior to cell division the flagellar microtubules depolymerize and the flagella shorten. 4. The TZ detaches from the basal body (BB) forming a vesicle inside the flagellar collar (C). The transitional fibers (TF), which attach the basal body to the membrane, are not a part of the TZ. C-E. Transition zones are trapped in flagellar collars of isolated cell walls. C. Isolated cell walls retain pairs of flagellar collars (left panel, arrows) many of which contain a punctum of acetylated α -tubulin (center panel, arrows). D. In an end-on view, a TZ is seen in the center of each flagellar collar. E. CEP290, a protein known to be associated with the TZ in situ, is also present in many of the shed TZs.

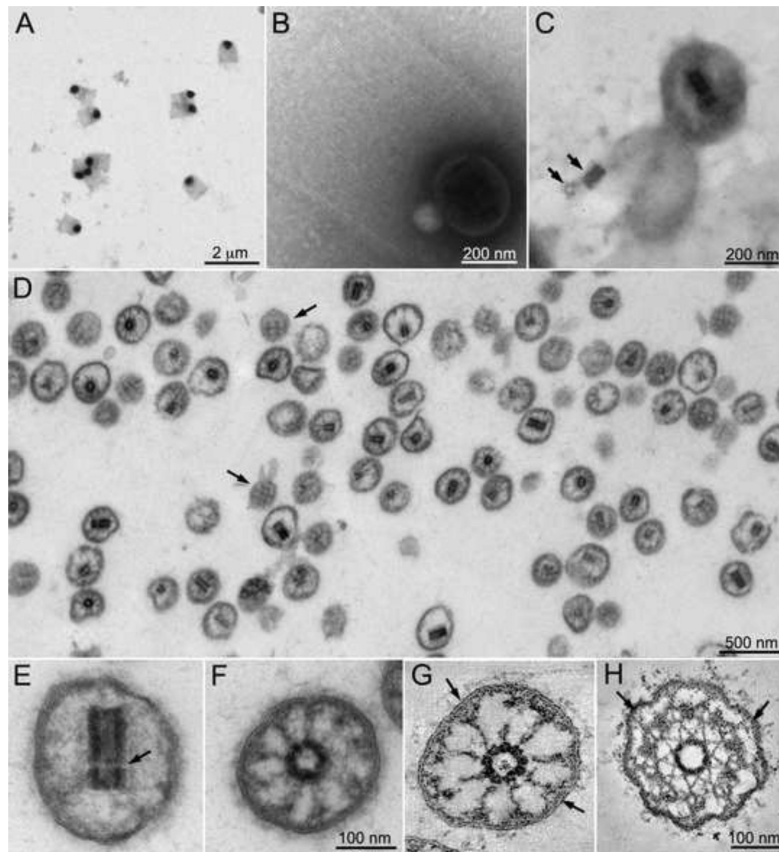


Figure 2.

Electron microscopy of isolated TZs. A. Negative stain electron microscopy of a band from a cesium chloride gradient of isolated cell walls reveals flagellar collars containing an electron dense vesicle. B. At higher magnification fibers of the flagellar collar can be seen entrapping the vesicle. C. After detergent treatment of the grid, the central cylinder characteristic of the TZ is seen inside the vesicles. The lower vesicle has lysed releasing the central cylinder, which separated into its proximal and distal components (arrows). D. Purified TZs, identified by the presence of the central cylinder in medial sections, are seen by electron microscopy of a section through a pellet of material fractionated on an iodixanol gradient. Tangential sections of TZs reveal a crosshatching of electron dense material on the inner surface of the membrane (arrows). E. In longitudinal section the distal and proximal sections of the central cylinder are visible although the transverse plate is missing (arrow). F. In cross section, although the microtubules had depolymerized, attachments can be seen between the central cylinder and the membrane. G and H: Virtual 6 nm sections of tomographic reconstructions of a TZ after isolation (G) or in situ (H). Y-shaped connectors can be seen between the outer doublet microtubules and the membrane in the TZs in situ (H, arrows). The Y-shape can sometimes be seen in the membrane attachments in the isolated TZs (G, arrows). See also Figs. S1 and S2 and Movie S1.

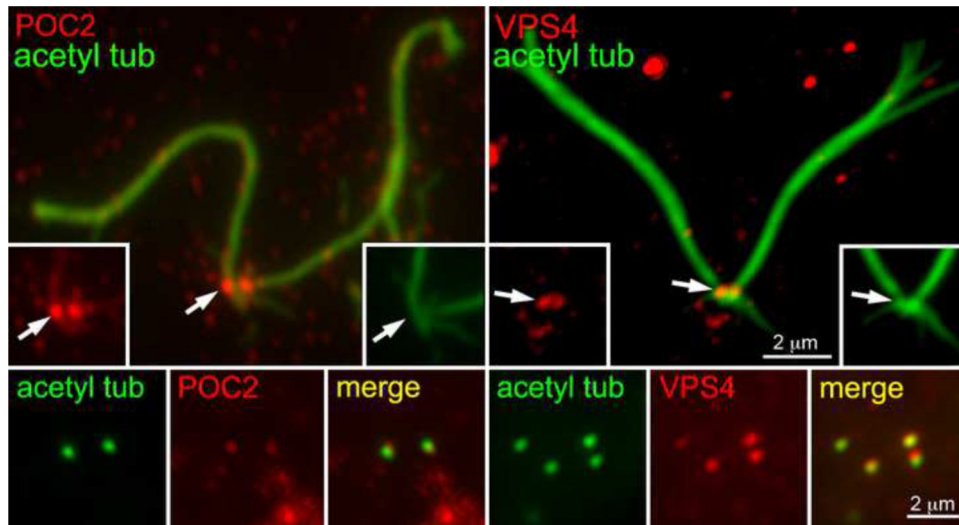


Figure 3. POC2 and VPS4 are localized at the TZ. Isolated flagella/basal body complexes (upper panels) stained for acetylated α -tubulin (green) show a pair of POC2 (left, red) and VPS4 (right, red) puncta at their base. Immunostaining of TZs in isolated cell walls (lower panels) confirms the presence of POC2 and VPS4 in the TZ.

Table 1

Newly identified proteins in the TZ and related human proteins.

Protein	Type/Motif^a	<i>Chlamydomonas</i>	<i>Homo sapiens</i>	e-value
POC2	PLAT	XP_001690405	NP_653213	1e-141
MOT51	PLAT, HELP, WD40	XP_001703421	NP_653213	4e-127
VPS28	ESCRT-I	XP_001695966	NP_057292.1	1e-40
VPS23	ESCRT-I	XP_001692483	AAH02487.1	8e-42
VPS37	ESCRT-I	XP_001696016	NP_001138624.1	1e-8
VPS60	ESCRT-III	XP_001693548	NP_001182465.1	9e-39
VPS4	ESCRT - Vps4	XP_001701670	NP_004860.2	3e-170
PDCD6IP	ESCRT-related, Bro1, Alix	XP_001702137	AAK20398.1	1e-44
ALA2	ATPase-Plipid, flippase	XP_001692884	NP_057613.4	0
CYCA1	A-type cyclin	XP_001693167	AAB60863.1	3e-67
CDKA1	Cyclin dependent kinase	XP_001698637	NP_001249.1	1e-137
DNA damage inducible protein	RP_DDI, UBQ, UBA	XP_001698476	CAD67552.1	3e-61
DM10 domain-containing protein	DUF1126	XP_001698964	NP_060570.2	2e-72
FOX1	Multicopper ferroxidase	XP_001694585	EAX05385.1	1e-156
Predicted protein	C2	XP_001699936	BAF82219.1	2e-11
Predicted protein	CDC50, LEM3	XP_001695413	NP_001017970.1	7e-44
Predicted protein	Dzip-like_N, ApoLp-III_like	XP_001689748	AAH33308.1	9e-16
Predicted protein	Leucine-rich repeats	XP_001692815	CAB07532.1	3e-33

Also see Tables S1-S4.

^aMotifs were taken from the NCBI gene page.